

Gait-based Authentication using Trousers Front-Pocket Sensors

Shinsuke Konno^{*}, Yoshitaka Nakamura^{**}, Yoh Shiraishi^{**}, and Osamu Takahashi^{**}

^{*} National Institute of Technology, Hakodate Collage, Japan

^{**} School of Systems Information Science, Future University Hakodate, Japan

skonno@hakodate-ct.ac.jp

{y-nakamr, siraisi, osamu}@fun.ac.jp

Abstract - Recently, to reduce the inconvenience caused by authentication operations in portable terminals, various authentication methods based on behavior characteristics have been studied. Gait-based authentication is one of them. This authentication method identifies individuals based on walking motions measured by wearable sensors such as acceleration sensors. This study aims to improve the authentication accuracy using trouser front pocket sensors. In this study, we consider two analyses to achieve this goal. First, we investigate the relation between walking motion and gait signals from trouser pocket sensors to extract signals of same-gait motion intervals in different subjects. Next, we verify an authentication method that uses both an acceleration sensor and a gyro sensor to improve the authentication accuracy.

Keywords: gait-based authentication, acceleration sensor, gyro sensor, dynamic time warping, fusion

1 INTRODUCTION

The use of portable terminals such as smartphones has increased in the various situations and can be expected to increase in the future. Accordingly, smartphones and other portable terminals have equipped various personal authentication functions to prevent imposters from misusing. Recently, authentication functions such as pattern locks, which are more difficult for an imposter to break, has been incorporated into the devices. However, there are reports and news items showing that approximately 50% of users do not lock their devices by inconvenient their operations.

Previous studies proposed easier authentication methods by various device operations, such as swinging their terminals. However these methods require conscious action, so they cannot perform authentication in the background.

On the other hand, it is conceivable that individual authentication might be established through daily repeated activities. With such a method, a user can unlock a terminal without conscious operations. Gait-based authentication is one of this type authentications. We think that walking is performed in various situations. If gait authentication was established by sensors on a portable terminal, the inconvenience users feel in individual authentication would be reduced.

We work with multi-modal authentication to improve authentication performance by combining multiple methods in individual authentication [1]. Fernand et al. [2] combined faces and fingerprints to improve accuracy. Zhou et al. [3] combined features of side face and gait using principal component analysis to identify people, and many other

researchers have also attempted to improve accuracy using biometric authentication.

However, wearing multiple sensors on various body parts sacrifices convenience, the advantage of gait authentication. For this reason, we adopt a method that combines multiple sensor methods measuring the same body parts using multiple sensors, and a multi-sample method that measures a modality several times to improve performance. It is possible to equip a terminal with multiple sensors, enabling us to authenticate using multiple sensors without imposing a burden on users.

In this study, we use two sensors (a three-axis acceleration sensor and a three-axis gyro sensor) to measure human walking motion. We show that the proposed method, which combines distance information recorded by these two sensors, improves authentication accuracy in comparison with previous studies.

2 RELATED WORK

2.1 Position of sensors

Table 1 summarizes the related work. These studies explored features and authentication methods primarily to improve performance. However, they did not investigate which sensor positions would be acceptable for daily use.

Those studies measured mainly using devices attached on the belt on the middle or side of the waist, and authenticated using measured acceleration signals. This requires using a smartphone case such as a holster for attaching the terminal to the waist. Users might find this unacceptable, because gait authentication then requires them to have the container with them. Consequently, we decided that the trouser front-pocket might be acceptable to users, because they can then have the terminal without using special tools, and we investigated performance improvement in this position. The study in [6] examined this position. This study aims to improve authentication performance in comparison to that previous study.

Table 1: Summary of gait-based authentication work

work	position	Sensor
Mäntyjärvi et al. [4]	belt	acceleration
Gafurov et al. [5]	hip	acceleration
Gafurov et al. [6]	ankle	acceleration
Gafurov et al. [7]	trouser pocket	acceleration
Gracian et al. [8]	belt	acceleration
Derawi et al. [9]	belt	acceleration
Soumik et al. [10]	eight-joints	rotation angle

2.2 Fusion of multiple sensors

Many acceleration-based approaches to gait-based authentication have been explored.

Mäntyjärvi et al. [4] proposed three authentication methods: fast Fourier transform, correlation, and statistical features. Gafurov et al. [5][6][7] studied methods based on acceleration, and made measurements by using acceleration sensors on various parts of subject's bodies. They used a template signal and multiple time-normalized signals, with the acceleration sensor placed in the trouser front pocket [7].

Gracian et al. [8] devised the feature of gait acceleration for user authentication. Derawi et al. [9] proposed a multi-sampling method that authenticated using multiple signals from both templates and inputs. Their method calculated distances of all combinations of templates and inputs with dynamic time warping (DTW). Soumik et al. [10] measured walking motions with eight angle sensors.

To the best of our knowledge, there are no studies on the fusion of multiple sensors placed in a trouser front pocket. To improve authentication accuracy, we propose a method of fused distances based on acceleration and angular velocity placed in a trouser front pocket.

3 PROPOSED METHOD

3.1 Gait recognition and quasi-periodic signal extraction

We attached a sensor unit whose x-, y-, and z-axis detected vertical, sideway, and forward-backward acceleration, respectively, in standing posture. The direction of each axis is shown in Figure 1. Each subject wore a sensor unit attached to a belt with hook and loop fastener. This unit was placed on the front of the left femur area.

Examples of three-axis acceleration and three-axis angular velocity are shown in Figures 2 and 3. During walking, the acceleration and gyro sensors measured similar waveforms repeatedly. These signals are quasi-periodic signals with no equalization of cycles and amplitudes.

The length of a gait cycle is two steps. The gait cycle consists of four periods, two double limb support periods, and two single limb support periods. We walk forward by repeating the four periods. If we extract the gait signals from different walking period for each subject, we may achieve good performance seemingly in authentication. To prevent influence on authentication accuracy by different waveform for each user, we decided to extract their quasi-periodic signals with the same order of the gait periods to all users. For this reason, we conducted a preliminary experiment to investigate the relation between walking motion and six-axis signals. Two force sensors synchronized with the sensor unit were attached to their left toe and heel. Examples of the acceleration along the x-axis and the signal of the force sensor are shown in Figure 4. The graph shows that the time when the acceleration becomes a local maximum is approximately equal to the time when the value of the heel force sensor begins to increase. This result indicates that the time of local maximum of acceleration is the heel landing time.

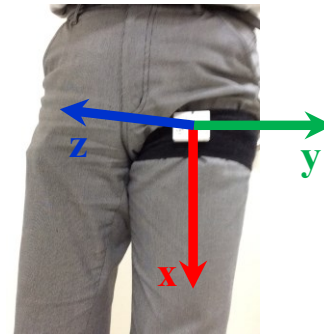


Figure 1: Directions of three axes.

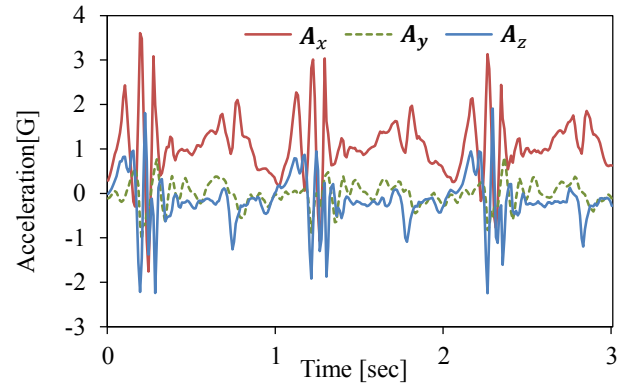


Figure 2: Gait signals from three-axis acceleration sensor.

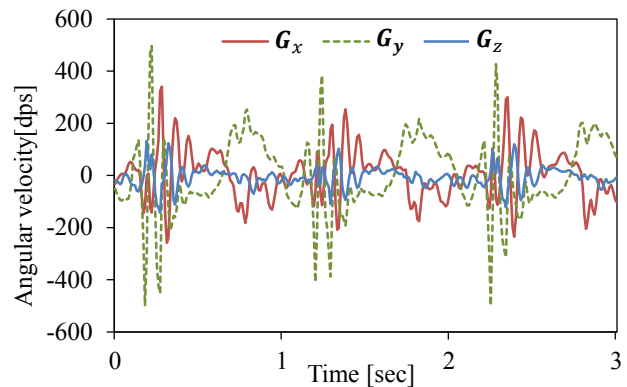


Figure 3: Gait signals from three-axis gyro sensor.

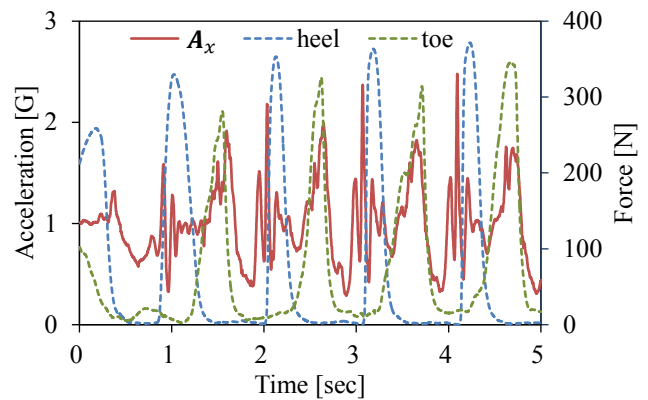


Figure 4: Example of the vertical acceleration signal and force signal.

3.1.1. Walking detection

In this study, we use a threshold in vertical acceleration to detect walking start time based on previous research [7]. Before beginning, all signals were smoothed using a Savitzky–Golay filter [11]. We look for the time t_s when the acceleration is greater than 1.2 G from the start of this quasi-periodic signal extraction method.

3.1.2. Quasi-periodic signal extraction

After walking detection, we extract quasi-periodic signals measuring the period between left-heel landing time. The extraction process with x-axis acceleration A_x is as follows:

- 1) We search for the maximum time T_0 within two seconds after t_s . We selected T_0 as the start time of cycle C_0 .
- 2) To find the end time of C_0 , we search for all times of local maxima from 0.7 to 1.3 s after T_0 from A_x .
- 3) We extract subsets s_0 that are 0.6 s of the signal. T_0 is the middle time of subset s_0 . In the same way, each t_1 is the middle time of subsets $S_1 = \{s_{11}, s_{12}, s_{13} \dots\}$, which are extracted as 0.6 s signals. We calculate values of the normalized cross correlation (NCC) among s_0 and each S_1 . The middle time of NCC values is decided as the start time T_1 of the next cycle C_1 . Cycle C_0 is between T_0 and T_1 . This is shown in Figure 5.
- 4) Next, we search for all times of local maxima from 0.7 to 1.3 s after T_1 . We extract the subsets of signal from T_1 to each time of the local maxima. The time of minimum distance among C_0 and each subset with DTW is decided as the start time T_2 of the next cycle C_2 . In this calculation, to eliminate the effect of differences in signal length, we divided each distance by the total length of C_0 and each S_2 .
- 5) After the time T_n of minimum distance is calculated using DTW among C_{n-1} and S_n , we begin searching for the next start time T_{n+1} by repeating step 4).
- 6) When forward searching is completed, we repeat the process by searching backward at T_0 .
- 7) When we observed the extracted signals, we found that those near the signals of starting to walk had a large distortion as compared with other signals. Based on the result of analysis, the variance of each signal with a large distortion is smaller than the variance of other signals. Hence, we searched for the first distorted signals whose variance was greater than the threshold 0.09. We assumed that the signals used for authentication were signals subsequent to it. Examples of the variance from extracted signals are shown in Figure 6. In this x-axis acceleration, we took the signals to be used for authentication as the cycles after C_0 . We recorded the starting times of extracted cycles, and extracted signals for the other two-axis acceleration and three-axis angular velocity using the same starting time.

Figure 7 shows two extracted signals from the same subject. In Figure 8, the two lines indicate extracted signals from different subjects.

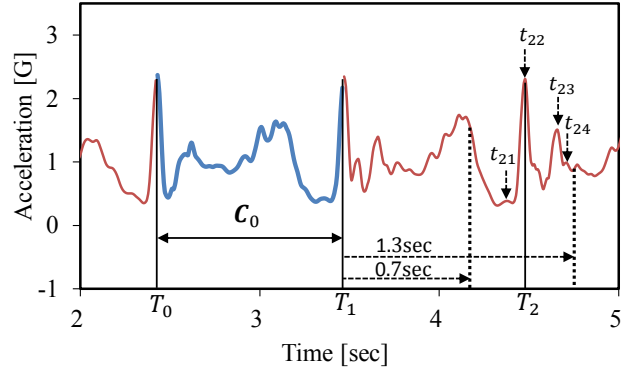


Figure 5: Example of extracted cycle C_0 and local maximum.

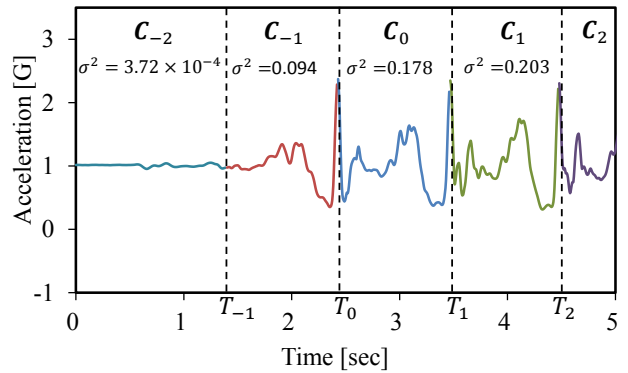


Figure 6: Example of extracted cycles and their variances.

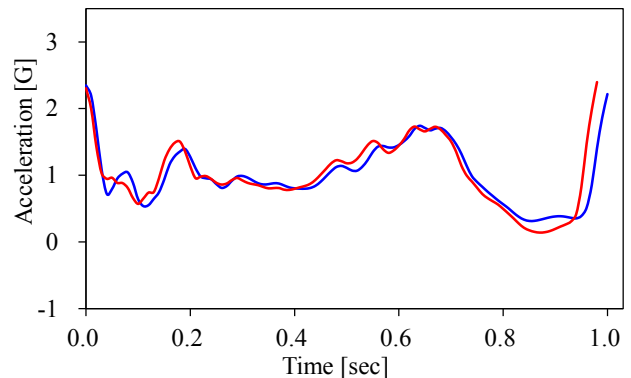


Figure 7: Extracted signals from same subject.

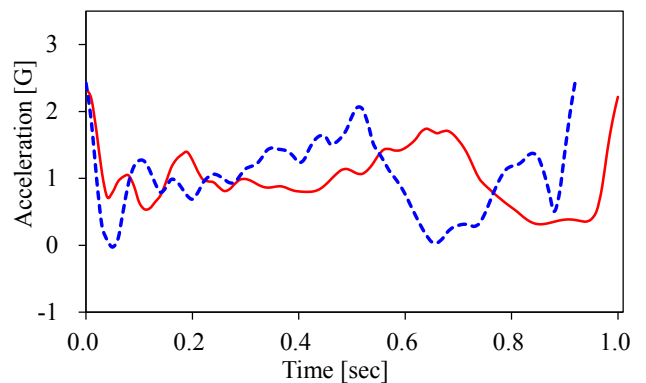


Figure 8: Extracted signals from two subjects.

3.2 Distance calculation methods

We selected DTW that is frequently used for calculating dissimilarity between time series data. Let $\mathbf{X} = \{x(i)|i = 1, 2, \dots, m\}$, $\mathbf{Y} = \{y(j)|j = 1, 2, \dots, n\}$ be time series data. The DTW distance between \mathbf{X} and \mathbf{Y} is defined as

$$\begin{aligned} DTW(\mathbf{X}, \mathbf{Y}) &= f(m, n) \\ f(i, j) &= \min \begin{cases} f(i-1, j-1) + dist(x(i), y(j)) \\ f(i, j-1) + dist(x(i), y(j)) + GP \\ f(i-1, j) + dist(x(i), y(j)) + GP \end{cases} \\ f(0, 0) &= 0 \end{aligned}$$

where $DTW(\mathbf{X}, \mathbf{Y})$ is the DTW distance, m and n are the number of lengths in signals \mathbf{X} and \mathbf{Y} , and GP is a gap penalty in the case of non-linear extension. We adopted the different distance calculation method for each sensor. The distance calculation function is substituted into $dist(x(i), y(j))$ corresponding to the type of sensors. Next, to adapt the differences of signal length to differences of walking speed, Normalized distance $D(\mathbf{X}, \mathbf{Y})$ is calculated as

$$D(\mathbf{X}, \mathbf{Y}) = \frac{DTW(\mathbf{X}, \mathbf{Y})}{m + n}$$

In the multi-sample case, we used the median as the distance. Let $\mathbf{Y} = \{\mathbf{Y}_1, \mathbf{Y}_2, \dots, \mathbf{Y}_k, \dots, \mathbf{Y}_p\}$ be multiple template signals. This distance was calculated as

$$D(\mathbf{X}, \mathbf{Y}) = \text{median}_k(D(\mathbf{X}, \mathbf{Y}_k))$$

where $D(\mathbf{X}, \mathbf{Y}_k)$ is the normalized distance between an input signal and k template signals of multiple template signals.

3.2.1. Angular velocity distance

It is known that angular velocity does not depend on distance from the center of rotation. We calculate the absolute distance between the input signal and template signals. Even if signals of the same subject are selected, they do not correspond to the amplitude value from a difference in walking speed. To reduce differences between signals of the same subject, we normalized the signals by dividing the amplitude of each time by specific values. We adopted the method of normalization that divides amplitude of signal by the root mean square (RMS). The reason for using RMS for normalization is that it provided the best accuracy among some normalized methods in a preliminary experiment.

Let $\mathbf{g}_{in}^q = (g_{in}^q(1), g_{in}^q(2), \dots, g_{in}^q(i), \dots, g_{in}^q(m))$ be the q-axis input angular velocity signal, and let $\mathbf{g}_{t_k}^q = (g_{t_k}^q(1), g_{t_k}^q(2), \dots, g_{t_k}^q(j), \dots, g_{t_k}^q(n))$ be the q-axis k template angular velocity signal. We calculate the difference of the composed angular velocity between the i^{th} amplitude of a q-axis input angular velocity signal and the j^{th} amplitude of a q-axis k template angular velocity signal by the absolute distance as

$$dist(g_{in}^q(i), g_{t_k}^q(j)) = |g_{in}^q(i) - g_{t_k}^q(j)|$$

3.2.2. Acceleration distance

When measuring circular motion, it is known that acceleration depends on the distance from the center of rotation. If different amplitude normalizations are applied to each axis acceleration, they are compressed at different ratios at the same time. As a result, when the normalized accelerations of the three axes at the same time were combined as a vector, the direction of the vector was changed before normalization. This problem was caused by comparing it with the values of acceleration. Hence, we compared it with the direction of three-axis acceleration between the input and the template acceleration signals [12].

Let $\mathbf{a}_{in}(i) = (a_{in}^x(i), a_{in}^y(i), a_{in}^z(i))$ be the i^{th} input acceleration vector of an input signal, and let be $\mathbf{a}_{t_k}(j) = (a_{t_k}^x(j), a_{t_k}^y(j), a_{t_k}^z(j))$ be the j^{th} template acceleration vector of a k template signal. We calculate the difference of direction between the i^{th} input acceleration vector and j^{th} k template acceleration vector as

$$dist(\mathbf{a}_{in}(i), \mathbf{a}_{t_k}(j)) = \arccos \frac{\langle \mathbf{a}_{in}(i), \mathbf{a}_{t_k}(j) \rangle}{\|\mathbf{a}_{in}(i)\| \|\mathbf{a}_{t_k}(j)\|}$$

To compare this three-axis composite method with others, authentication accuracy of each axis acceleration was calculated based on same distance calculation method for angular velocity.

3.3 Distance fusion

To eliminate subject dependency, we subtracted the average distance from the distance before fusion. This average distance was calculated between a subject's template signal \mathbf{Y} and the same subject's training data γ except his or her template signal \mathbf{Y} . The normalized distance is calculated by subtracting the average distance from the distance calculated by DTW between an input signal and the template signals as

$$D_s(\mathbf{X}, \mathbf{Y}) = D(\mathbf{X}, \mathbf{Y}) - \overline{D(\gamma, \mathbf{Y})}$$

Finally, we calculated the fused distances D_f as

$$D_f = f(D_s(\mathbf{a}_{in}, \mathbf{a}_t), D_s(\mathbf{g}_{in}^x, \mathbf{g}_t^x), D_s(\mathbf{g}_{in}^y, \mathbf{g}_t^y), D_s(\mathbf{g}_{in}^z, \mathbf{g}_t^z))$$

where $f()$ is a function of fusion which combines the distances.

In this study, we consider four rules for fusing distances for authentication (1) Addition without weight coefficients (denoted as Sum), (2) Linear logistic regression (denoted as LLR), (3) Support vector machine (SVM) with linear kernel (Linear), (4) SVM with a radial basis function kernel (RBF)

In this study, we obtained too many negative instances as compared with positive instances. It is well known that SVM performs poorly in this case. Hence, we applied the synthetic minority over-sampling technique [13] to adjust the number of these instances.

4 EXPERIMENT

4.1 Dataset

Data was collected from 50 subjects, ranging in age from 18 to 21 years old. We instructed the subjects to walk at their normal walking speeds. When the measurement began, the subjects remained stationary for a few seconds. After that, they walked a specified distance once. The measurement course is a flat and straight indoor passageway. The subjects did not use a clock or metronome to measure their walking speed. We set the sampling frequency of the sensor unit to 1,000 Hz. To equalize the performance of the smartphone's sensors, we changed the sampling frequency from 1,000 to 100 Hz by thinning out.

4.2 Experimental setting

We obtained 30 signals of each axis acceleration and 30 signals of each axis angular velocity from every subject. We divided the signals into five groups and performed five-fold cross-validation. To generate a fusion model, we used four groups as training data, and one group as test data. We calculated the distances between all of the training signals of all subjects. The distances between the same subjects are positive instances, and the distances between different subjects are treated as negative instances. The overall accuracies were calculated with common thresholds to each classifier in each fusion rule.

Template signals used for calculating distance include six signals, because the number of template signals is equal to the number of template signals of the previous study [7]. The manner of selecting templates from training data was to select six sequential signals from 24 signals. However, when some of the sequential six signals were selected as test data by cross-validation, we selected the signals in sequence from the nearest start time in the training data.

4.3 Experimental result

We evaluated accuracy by equal error rate (EER). The EER is the value when the false acceptance rate (FAR) and the false rejection rate (FRR) are the same. For comparison purposes, we calculated EERs four combinations of each method, and previous work distance calculation method [7].

We summarized the EERs in Tables 2 and 3. By comparing with each combinations, we can find that both multi-sensor and multi-sample are effective for accuracy improvement. The minimum EER (the best result) was 1.0%, which was achieved by the proposed multi-sensor multi-sample method with two SVMs.

Figures 10 show the receiver operating characteristics (ROC) curves for each authentication combinations. From the ROC curves, proposed method which is combination method with multi-sensor and multi-sample shows the best performance, because most of multi-sample with RBF line is plotted in the lower error rate area. The best EER from previous work method [6] to each axis signal for this dataset was 7.8%.

5 CONCLUSION

This paper describes an authentication method using multi-sampling and multi-sensors to improve the accuracy of gait-based authentication.

First, we observed the relation among the steps and six-axis signals in order to extract the quasi-periodic signals generated by walking motion of the same phase order in all subjects. These findings show that it is possible to divide into quasi-periodic signals by extracting x-axis acceleration from local maxima to local maxima.

We evaluated the proposed method with 50 subjects. The best EER performance was 1.0%, which was achieved by the multi-sensor multi-sample method using SVM. These results indicate that the combination of multi-sensor and multi-sample is useful for gait-based authentication. Furthermore, proposed method leads to better results than the conventional method.

Table 2: Uni-sensor EERs [%].

	Uni-sensor uni-sample authentication	Uni-sensor multi-sample authentication
a^x	8.8	4.5
a^y	5.3	2.2
a^z	4.6	2.2
g^x	6.6	2.4
g^y	8.2	3.1
g^z	7.4	3.0

Table 3: Multi-sensor EERs [%]

	Multi-sensor uni-sample authentication	Multi-sensor multi-sample authentication
Sum	1.7	1.2
LLR	1.5	1.1
Linear	1.5	1.0
RBF	1.4	1.0

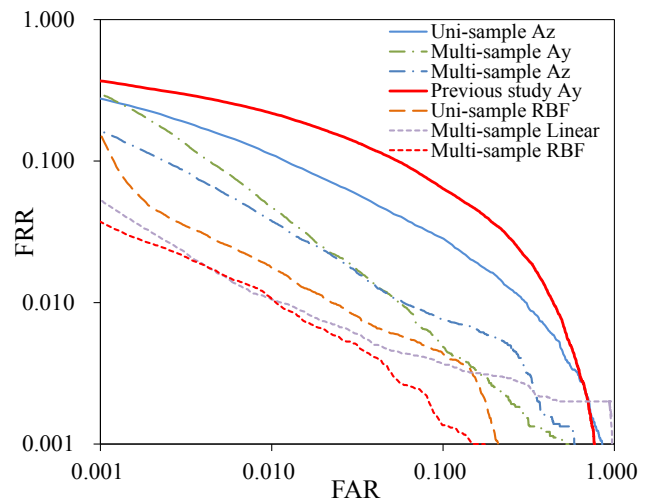


Figure 10: ROC curves of the best methods in each authentication combinations

REFERENCES

- [1] A.K. Jain, A. Ross, and S. Prabhakar, An Introduction to Biometric Recognition, IEEE Trans. Circuits and Systems for Video, Vol.14, No.1, pp.4-20 (2004).
- [2] F. Alonso-Fernandez, J. Fierrez, D. Ramos, and J. Ortega-Garcia, Dealing with sensor interoperability in multi-biometrics: The UPM experience at the Biosecure multimodal Evaluation 2007, Proc. of SPIE Defense and Security Symposium, Workshop on Biometric Technology for Human Identification, pp.69440J-69440J (2008).
- [3] X. Zhou and B. Bhanu, Feature Fusion of Side Face and Gait for Video-based Human Identification, Pattern Recognition, Vol.41, pp.778-795(2008).
- [4] J. Mäntyjärvi, M. Lindholm, E. Vildjiounaite, S. Mäkelä, and H.A. Ailisto, Identifying Users of Portable Devices from Gait Pattern with Accelerometers, Proc. of the IEEE International Conference on Acoustics, Speech and Signal Processing, pp.973-976 (2005).
- [5] D. Gafurov, E. Sneekenes, and T.E. Buvarp, Robustness of Biometric Gait Authentication Against Impersonation Attack, Proc. of the 1st International Workshop on Information Security (IS'06), OnTheMove Federated Conferences (OTM'06), Vol.4277, pp.479-488 (2006).
- [6] D. Gafurov, K. Helkala, and T. Sondrol, Biometric Gait Authentication Using Accelerometer Sensor, Journal of Computers, Vol.1, No.7, pp.51-59(2006).
- [7] D. Gafurov, E. Sneekenes, and P. Bours, Gait Authentication and Identification using Wearable Accelerometer sensor, Proc. of IEEE Workshop on Automatic Identification Advanced Technologies, pp.220-225(2007).
- [8] G. Trivino, A. Alvarez-Alvarez, and G. Bailador, Application of the Computational Theory of Perceptions to Human Gait Pattern Recognition, Pattern Recognition, Vol.43, pp.2572-2581(2010).
- [9] M.O. Derawi, P. Bours, and K. Holien, Improved Cycle Detection for Accelerometer Based Gait Authentication, Proc. of the 6th International Conference on Intelligent Information Hiding and Multimedia Signal Processing (IIH-MSP '10), pp.312-317(2010).
- [10] S. Mondal, A. Nandy, P. Chakraborty, and G.C. Nandi, Gait Based Personal Identification System Using Rotation Sensor, Journal of Emerging Trends in Computing and Information Sciences, Vol.3, No.3, pp.395-402(2012).
- [11] A. Savitzky and M.J.E. Golay, Smoothing and Differentiation of Data by Simplified Least-squares Procedures, Anal. Chem., Vol.36, No.8, pp.1627-1639 (1964).
- [12] F. Okumura, A. Kubota, Y. Hatori, K. Matsuo, M. Hashimoto, and A. Koike, A Study on Biometric Authentication based on Arm Sweep Action with Acceleration Sensor, Proc. of International Symposium on Intelligent Signal Processing and Communications, 2006(ISPACS '06). International Symposium on, pp.219-222(2006).
- [13] N.V. Chawla, K.W. Bowyer, L.O. Hall, and W.P. Kegelmeyer, SMOTE: Synthetic Minority Over-sampling Technique, Journal of Artificial Intelligence Research, Vol.16, pp.321-357(2002).